Development 139, 1777-1787 (2012) doi:10.1242/dev.079947

The role of hair cells, cilia and ciliary motility in otolith formation in the zebrafish otic vesicle

Georgina A. Stooke-Vaughan[1], Peng Huang[2], Katherine L. Hammond[1,*], Alexander F. Schier[2] and Tanya T. Whitfield[1,‡]

SUMMARY

Otoliths are biomineralised structures required for the sensation of gravity, linear acceleration and sound in the zebrafish ear. Otolith precursor particles, initially distributed throughout the otic vesicle lumen, become tethered to the tips of hair cell kinocilia (tether cilia) at the otic vesicle poles, forming two otoliths. We have used high-speed video microscopy to investigate the role of cilia and ciliary motility in otolith formation. In wild-type ears, groups of motile cilia are present at the otic vesicle poles, surrounding the immotile tether cilia. A few motile cilia are also found on the medial wall, but most cilia (92-98%) in the otic vesicle are immotile. In mutants with defective cilia (*iguana*) or ciliary motility (*lrrc50*), otoliths are frequently ectopic, untethered or fused. Nevertheless, neither cilia nor ciliary motility are absolutely required for otolith tethering: a mutant that lacks cilia completely (MZ*ovl*) is still capable of tethering otoliths at the otic vesicle poles. In embryos with attenuated Notch signalling [*mindbomb* mutant or *Su(H)* morphant], supernumerary hair cells develop and otolith precursor particles bind to the tips of all kinocilia, or bind directly to the hair cells' apical surface if cilia are absent [MZ*ovl* injected with a *Su(H)1+2* morpholino]. However, if the first hair cells are missing (*atoh1b* morphant), otolith formation is severely disrupted and delayed. Our data support a model in which hair cells produce an otolith precursor-binding factor, normally localised to tether cell kinocilia. We also show that embryonic movement plays a minor role in the formation of normal otoliths.

KEY WORDS: Zebrafish, Otic vesicle, Otoliths, Cilia, *atoh1b*, *igu*, *lrrc50*, *mib*, *ovl*

INTRODUCTION

Otoliths (in teleost fish) and otoconia (in mammals) are biomineralised structures that form inside the inner ear. They lie over patches of sensory hair cells, where they provide an inertial mass load for sensing gravity and linear acceleration. In fish, otoliths are also used for hearing (Popper and Fay, 1999; Popper and Lu, 2000; Abbas and Whitfield, 2010). In the zebrafish embryo, otolith formation begins immediately after the otic placode cavitates to form the otic vesicle (OV) at the 18 somite stage (18S) (Riley et al., 1997). Otoliths originate as dense, sticky precursor particles, which are initially distributed throughout the OV lumen. These nucleate directly over the developing sensory patches at the anterior and posterior OV poles to form two otoliths, a process that is robust and reproducible (Riley et al., 1997). After aggregation of precursor particles, otoliths become biomineralised by the crystallisation of calcium carbonate, stabilised by a protein and glycoprotein matrix, at ~26S.

Cilia have been implicated in otolith formation and positioning. These organelles are present on the apical surface of most vertebrate cells and are involved in sensory, signalling and mechanical processes (Bisgrove and Yost, 2006; Ishikawa and Marshall, 2011). Every cell of the zebrafish OV epithelium is monociliated (Riley et al., 1997), and many genes involved in ciliogenesis, intraflagellar transport, ciliary movement, stability and function are expressed in the OV (Tsujikawa and Malicki, 2004; Bisgrove et al., 2005; Omori and Malicki, 2006; Pathak et al., 2007; Omori et al., 2008; Sullivan-Brown et al., 2008; van Rooijen et al., 2008; Yu et al., 2008; Colantonio et al., 2009; Wilkinson et al., 2009; Gao et al., 2010; Glazer et al., 2010; Kang et al., 2010; May-Simera et al., 2010; Becker-Heck et al., 2011; Clément et al., 2011; Pathak et al., 2011; Ravanelli and Klingensmith, 2011; Rothschild et al., 2011; Yu et al., 2011). Sensory hair cells in the ear each bear a specialised cilium known as the kinocilium. Otolith precursor particles become tethered to the tips of the kinocilia on the first sensory hair cells that form in the ear; these cells are thus also known as tether cells, and their kinocilia as tether cilia (Fig. 1A) (Haddon and Lewis, 1996; Riley et al., 1997; Tanimoto et al., 2011).

There have been several conflicting reports of ciliary motility in the zebrafish OV and its role in otolith formation. By observing the non-Brownian movement of otolith precursor particles, Riley and others originally inferred that most OV cilia are motile, acting to agitate the otolith precursor particles (Riley et al., 1997). Tether cilia were observed to be immotile, forming a stable platform for otolith nucleation (Riley et al., 1997) (Fig. 1A, Model 1). More recently, a high-speed video microscopy study suggested the opposite scenario (Colantonio et al., 2009). In this model, all OV cilia are immotile, apart from clusters of motile tether cilia at the OV poles (Colantonio et al., 2009) (Fig. 1A, Model 2). This view was later revised in an experimental and modelling study of hydrodynamics in the OV, which proposed that the polar cluster contains both immotile tether cilia and nearby motile cilia (Wu et al., 2011). A further study, using high-speed imaging and genetic evidence, supports the original Riley model (Yu et al., 2011).

To resolve the controversial roles of cilia in otolith development, we have examined otolith formation and ciliary motility in the zebrafish OV using high-speed video microscopy in both mutant

[1]MRC Centre for Developmental and Biomedical Genetics and Department of Biomedical Science, University of Sheffield, Sheffield, S10 2TN, UK. [2]Department of Molecular and Cellular Biology, Broad Institute/Center for Brain Science, Harvard Stem Cell Institute/Center for Systems Biology, Harvard University, Cambridge, MA 02138, USA.

*Present address: School of Life Sciences, University of Liverpool, Liverpool, L69 7ZB, UK
‡Author for correspondence (t.whitfield@sheffield.ac.uk)

Accepted 1 March 2012

and morphant lines. Our results support some aspects of the most recent models (Wu et al., 2011; Yu et al., 2011), but differ in other important respects (summarised in supplementary material Table S1). We confirm that tether cell kinocilia are immotile and that groups of motile cilia are present nearby at the OV poles. We find that only a few of the cilia on the medial wall of the OV are motile; the majority are immotile. Cilia and ciliary motility are not absolutely required for otolith tethering; in the absence of cilia, otoliths are still able to nucleate by binding directly to the hair cell apical surface. Hair cells, however, are essential for normal otolith nucleation, and are the likely source of an unidentified 'otolith precursor-binding factor'. We also show that embryonic movement plays a minor role in the formation of normal otoliths. These results clarify the roles of hair cells, cilia and ciliary motility in otolith formation and positioning.

MATERIALS AND METHODS

Animals

Zebrafish lines used were AB, London wild-type (LWT), *igu*^{tm79a}, *igu*^{ts294e} (Brand et al., 1996; Sekimizu et al., 2004; Wolff et al., 2004), *kei*^{m219} (Malicki et al., 1996; Whitfield et al., 1996), *lrrc50*^{hu255H} (van Rooijen et al., 2008), *mib*^{ta52b} (Jiang et al., 1996; Itoh et al., 2003), *ovl*^{tz288b} (Tsujikawa and Malicki, 2004; Huang and Schier, 2009), *slo*^{tu44c} (Granato et al., 1996), *Tg(βactin2:Arl13b-GFP)* (Borovina et al., 2010) and *Tg(pou4f3:mGFP)* (Xiao et al., 2005). All mutant embryos were homozygous for the mutant allele; in MZ*ovl*^{tz288b} mutants, both maternal and zygotic gene activity was disrupted (Huang and Schier, 2009). M*ovl*^{tz288b} embryos were mutant for the maternal *ovl* allele only. Genotyping for *ovl* was performed as described (Huang and Schier, 2009). Embryos were raised in E3 medium (5 mM NaCl, 0.17 mM KCl, 0.33 mM $CaCl_2$, 0.33 mM $MgSO_4$, 0.0001% Methylene Blue). Embryonic stages are given as hours post fertilisation (hpf) at 28.5°C or as somite stages (S) (Kimmel et al., 1995; Westerfield, 2000). All animal experiments in Sheffield conformed to UK Home Office regulations.

High-speed video microscopy and live imaging

Embryos were anaesthetised in 0.5 mM MS222 (3-aminobenzoic acid ethyl ester), mounted in 3% methylcellulose, coverslipped and imaged with a 100× oil objective and 1.6× zoom using bright field optics on an inverted compound microscope (Olympus). Images were recorded with a Basler camera at ~300 frames per second (fps) using VideoSavant software. Fiji (Image J) was used to adjust brightness and contrast, crop and label images and convert to .avi format. iSquint was used to convert to .mp4 format. Time-to-colour merge pictures were generated by opening six consecutive movie frames as layers in the GNU Image Manipulation Program (GIMP), using the 'colorify' tool to assign each layer a different colour, changing the mode of the top five layers to 'difference', and then flattening the image. Saturation of time-to-colour merge pictures was increased in Adobe Photoshop CS5. Live embryos and fixed samples were also imaged using differential interference contrast (DIC) optics using a BX51 compound microscope, Camedia camera (C-3030ZOOM) and CELL-B software (Olympus). Images in Fig. 6 were taken with a Zeiss AxioImager.Z1 microscope, AxioCam MRc camera and AxioVision software.

In situ hybridisation

Whole-mount in situ hybridisation was carried out as described (Hammond et al., 2003). Probes used were *stm* (Söllner et al., 2003) and *otomp* (Murayama et al., 2005).

Immunohistochemistry and FITC-phalloidin staining

Staining was carried out as described (Haddon and Lewis, 1996). Primary antibodies were anti-acetylated tubulin (Sigma T6739, 1:100) and anti-GFP (Torrey Pines Biolabs TP401, 1:500). Secondary antibodies were anti-mouse TRITC (Sigma T5393, 1:50) and anti-rabbit FITC (Sigma F9887, 1:200). FITC-conjugated phalloidin (Sigma P5282, 0.25%) was used to stain actin. Images were taken using a confocal microscope (Leica SP1 or Olympus FV1000).

Morpholino injection

Translation-blocking morpholinos were dissolved in water and injected into one- to four-cell embryos. The *atoh1b* morpholino (*atoh1b*MO) (Millimaki et al., 2007) was injected at 1 ng/nl (~5 nl per injection). The morpholino to both *Su(H)1* and *Su(H)2* transcripts [*Su(H)1+2*MO] (Sieger et al., 2003; Echeverri and Oates, 2007) was injected at 0.5 mM (~0.5 nl per injection).

Embryo motility experiments

To restrict embryonic movement, embryos were raised at 21°C from shield stage overnight (for ease of staging), dechorionated at 15-18S, embedded in 3% methylcellulose in a Petri dish, covered with E3 and incubated at 28.5°C. Otolith phenotypes were scored 28-30 hours later. Control embryos were not dechorionated and were allowed to develop in E3 alone. To raise embryos under constant agitation, embryos were placed at 2-3 hpf into 50 ml Falcon tubes containing 25 ml E3. Tubes were placed on a roller mixer at ~26.5°C (rolled embryos grew faster than embryos in Petri dishes at the same temperature, presumably owing to better aeration). Otolith phenotypes were scored at 30 hpf. Control embryos were grown in a Petri dish at 28.5°C.

RESULTS

The early zebrafish otic vesicle contains several different classes of cilia

The lumen of the zebrafish otic vesicle (OV) forms by cavitation of the otic placode, and starts to appear at the 18 somite stage [18S; 18 hours post fertilisation (hpf)]. We examined ciliogenesis in the OV during and after cavitation (Fig. 1; supplementary material Fig. S1). At 17S, tubulin expression was concentrated along the length of the otic placode, marking the onset of cavitation, whereas at 19S, just after cavitation, each cell had a single cilium projecting from its apical surface into the OV lumen (Fig. 1B; supplementary material Fig. S1) (Riley et al., 1997). At this stage, the medial wall of the vesicle was fully epithelialised, but the lateral wall was less well organised (Fig. 1C,D). By 21S, groups of cilia (about six) were evident at the anterior and posterior OV poles (Fig. 1B-E; supplementary material Fig. S1). These groups included a pair of cilia at each pole belonging to the first hair cells (tether cells), identified by their GFP expression in the *Tg(pou4f3:mGFP)* line at 25S (Fig. 1E; fixed sample). Between 20S and 25S, the number of cilia in the ear remained constant (~200; Fig. 1F). Initially, cilia throughout the ear were similar in length. As development proceeded, tether cell cilia remained long, but cilia on the medial and lateral OV walls, and non-tether cell cilia at the poles, regressed in length and were difficult to detect in fixed material by 29S (supplementary material Fig. S1) (Riley et al., 1997). However, imaging of live *Tg(βactin2:Arl13b-GFP)* embryos indicated that cilia were still present throughout the OV at 30 hpf (data not shown) (Borovina et al., 2010).

To observe ciliary motility, we used high-speed video microscopy at 300 frames per second (fps) to image ears from 18S to 25 hpf. Cilia on the lateral wall were always immotile (n=23 ears); in both AB and LWT wild-type strains, motile cilia were absent on lateral wall cells. By contrast, motile cilia were present both at the poles and on the medial wall of the OV lumen, which had between one and five motile cilia in addition to immotile cilia, at all stages observed (Fig. 2; supplementary material Movies 1-9). Ciliary movement was rotatory, with an estimated mean beat frequency of 28 Hz (s.d.=4.8) at 19-24S and 33 Hz (s.d.=5.9) at 24-25 hpf. In one example, we documented a cilium rotating first in one, and then in the opposite, direction (supplementary material Movie 6). Ears from LWT embryos had more motile cilia (both at the poles and on the medial wall) than those of the AB strain (Fig. 2I; two-tailed t-test, P=0.0166). However, the vast majority (92-98%) of otic cilia in both wild-type strains were immotile.

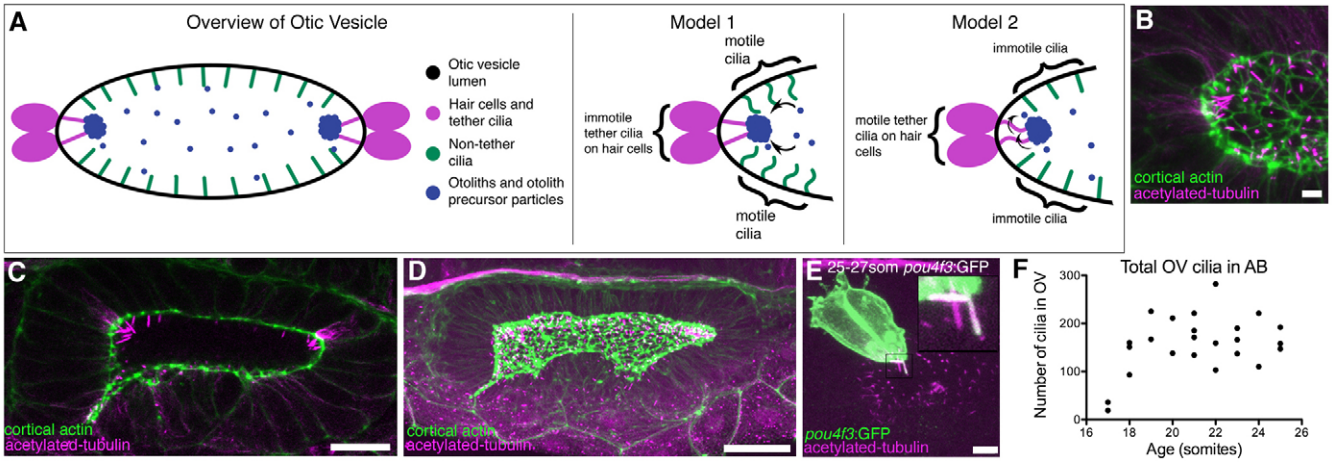

Fig. 1. Presence of cilia in the developing otic vesicle of wild-type zebrafish embryos. (**A**) Cartoon overview of 18-25S OV and illustrations of current models of otolith formation. (**B**) Confocal projection showing the anterior OV pole in a 21S embryo (lateral view), stained with FITC-phalloidin (green; cortical actin) and anti-acetylated tubulin (magenta). Scale bar: 5 µm. (**C**) Single confocal section showing clusters of cilia at the anterior and posterior poles in a 21S stage AB embryo (dorsal view). Scale bar: 20 µm. (**D**) Confocal projection of the whole OV in a 19-21S LWT embryo. Scale bar: 20 µm. (**E**) Anti-GFP and anti-acetylated tubulin stain of a *Tg(pou4f3:mGFP)* embryo. GFP marks the hair cells and their kinocilia. Tether cilia are double-labelled and appear white; other cilia are magenta (inset). Scale bar: 5 µm. (**F**) Scatter plot showing change in total number of cilia in the OV of AB wild-type embryos.

The groups of cilia at the poles of the vesicle consisted of both immotile and motile cilia. Hair cell kinocilia (tether cilia) were immotile, and became attached to otolith precursor particles as soon as the OV lumen opened (Fig. 2B). In addition, there were usually one to four motile cilia immediately surrounding the tether cells. These did not belong to hair cells [they were GFP-negative in the *Tg(pou4f3:mGFP)* line] (Fig. 1E; fixed sample), and did not tether the main otolith mass (supplementary material Movie 4). The vigorous movement of these cilia appeared to cause slight passive movement of the otolith and tether cilia (Fig. 2B,D; supplementary material Movies 2, 4). By 24 hpf, motile cilia at the poles had decreased in length and could be distinguished clearly from the longer immotile tether cilia attached to the otolith (Fig. 2G; supplementary material Movie 7).

Hair cell kinocilia are immotile, even in the absence of otolith binding

In most cases, the motile cilia at the OV poles did not bind to otolith precursor particles. However, in two examples, we saw a motile cilium attached to otolithic material (supplementary material Movie 8). This raised the possibility that otolith binding triggers a change in, or physically restricts, motility in the tether cilia. To test this, we examined ciliary movement in the *keinstein* (*kei*) mutant, in which otoliths never nucleate and grow (Whitfield et al., 1996). The gene disrupted in *kei* is currently unknown. Hair cells, tether cilia and non-tether cilia were present at all stages in *kei* mutant ears (Fig. 3). The tether cilia were easy to see, as they were not obscured by otolithic material and were immotile at all stages. Some small particles became attached to their tips, but otoliths never formed properly (Fig. 3A,D; supplementary material Movies 9, 10). Interestingly, the tether cilia in *kei* ears appeared longer than those in the wild type (supplementary material Fig. S2). We presume that this indicates that part of the kinocilium in a wild-type ear normally becomes embedded in the otolith, rather than the presence of a ciliary length defect in *kei*.

We conclude that all hair cell kinocilia, including the tether cilia, are always immotile (apart from small passive displacements), and that otolith binding does not result in a change in their motility. Although motile cilia occasionally bind otolith precursor particles, they do not tether the main otolith mass. Hair cells are continually added to the growing sensory patches, however, and we cannot rule out the possibility that neighbouring cells, initially with motile cilia, eventually give rise to hair cells with immotile kinocilia.

Otoliths can form in the absence of cilia and are able to nucleate correctly to the poles of the otic vesicle

To test the requirement for cilia in the process of otolith formation, we examined otolith development in MZ*ovl* mutants, which lack both maternal and zygotic *ift88* gene function and are completely devoid of cilia in all tissues, including the ear (Huang and Schier, 2009). Tether cells were present, but lacked cilia (Fig. 4A-C). Surprisingly, we found that otoliths were able to form in MZ*ovl* embryos, often in the correct number and position at the two OV poles (Fig. 4C,D). However, otolith formation was not completely normal. In MZ*ovl* mutants at 30 hpf, 69% (93/134) of ears had a posterior otolith that appeared to be a fusion of two smaller otoliths, 6% (8/134) of ears had an anterior otolith that appeared to be a fusion of two smaller otoliths, 9% (12/134) of ears had three separate otoliths, one of which was untethered, and 1% (2/134) of ears had an otolithic defect that did not fit into the previous categories (Fig. 4D). The remaining 14% (19/134) had two normal otoliths, which formed close to the apical surface of the epithelium (Fig. 4D). As controls, we examined M*ovl* mutants (heterozygous embryos lacking maternal *ift88* contribution but with normal zygotic *ift88* function); these had 100% normal otoliths (146/146; Fig. 4A,D).

We also examined otolith formation in the *iguana* (*igu*) mutant, which disrupts the function of *dzip1*, a gene required for ciliogenesis (Brand et al., 1996; Sekimizu et al., 2004; Wolff et al., 2004; Huang and Schier, 2009; Glazer et al., 2010; Kim et al., 2010; Tay et al., 2010). We found a variable loss of otic cilia in the two available alleles (igu^{tm79a} and igu^{ts294e}) but, contrary to a previous report (Yu et al., 2011), tether cell kinocilia were usually present (Fig. 4E-G) (and see supplementary figure S5 in Huang and Schier, 2009)

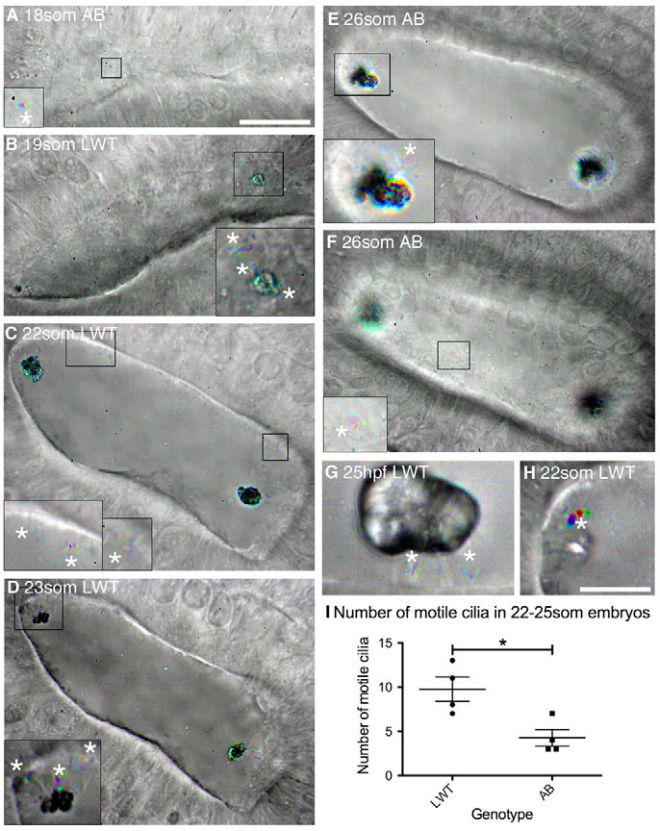

Fig. 2. Ciliary motility in the developing wild-type zebrafish otic vesicle. All panels are dorsolateral views of the left ear, with anterior to the right, and are merged time-to-colour composites of six consecutive frames of a high-speed movie. Grey scale shows lack of movement; colour indicates movement. White asterisks mark motile cilia. (**A**) 18S AB strain wild-type embryo with one motile cilium present on the medial wall (shown in inset). See supplementary material Movie 1. (**B**) 19S LWT wild-type embryo. Inset shows motile cilia next to the anterior otolith and movement of the anterior otolith. See supplementary material Movie 2. (**C**) 22S LWT wild-type embryo. Insets: motile cilia present on the medial wall of the OV (two in the left hand inset, one in the right hand inset). See supplementary material Movie 3. (**D**) 23S LWT wild-type embryo. The posterior otolith is shown on two immotile tether cilia (grey); three motile cilia are nearby (coloured). See supplementary material Movie 4. (**E**) 26S AB wild-type embryo. Inset: motile cilia next to posterior otolith. See supplementary material Movie 5. (**F**) Different focal plane of the embryo shown in E. One motile cilium was present on the medial wall of the OV (inset) that rotated first one way and then the other. See supplementary material Movie 6. (**G**) 25 hpf LWT wild-type embryo. The otolith sits on two to three tether cilia; two short, motile cilia remain directly underneath. See supplementary material Movie 7. (**H**) Very rarely, one or a few otolith precursor particles were bound to a motile cilium (asterisk; 22S LWT wild-type embryo). See supplementary material Movie 8. (**I**) Number of motile cilia found per OV in AB and LWT wild-type strains. Bars represent mean ± s.e.m.. Scale bars: 20 μm in A, for A-F; 10 μm in H, for G,H and insets in A-F.

(Huang and Schier, 2009). Like MZ*ovl*, mutants for both *igu* alleles formed otoliths, and in 58% (181/314) of cases these were normal: two otoliths formed, tethered in correct place, although sometimes closer to the apical membrane (Fig. 4G,H). Otolith abnormalities were observed in 42% (133/314) of embryos (Fig. 4H). These data suggest that cilia are not absolutely required for otolith formation, but are important to ensure its accuracy and robustness.

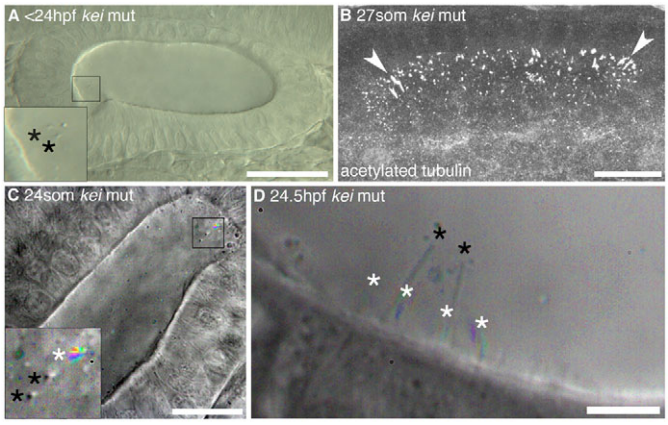

Fig. 3. Tether cilia are immotile even in the absence of otoliths. (**A**) DIC image of a <24 hpf *kei* mutant showing anterior tether cilia (inset, black asterisks) without any bound otolith, although otolith precursor particles are present. Scale bar: 40 μm. (**B**) Confocal stack through the OV of a 27S *kei* mutant embryo. Cilia appear normal (arrowheads indicate tether cilia). Scale bar: 20 μm. (**C**) Time-to-colour merge of six frames of a high-speed movie of a 24S *kei* mutant embryo. Inset: two immotile kinocilia (marked by black asterisks) and one motile cilium (marked by white asterisk). Scale bar: 20 μm. See supplementary material Movie 9. (**D**) Time-to-colour merge of six frames of a high-speed movie of a 24.5 hpf *kei* mutant embryo; kinocilia (black asterisks) are immotile. White asterisks mark motile cilia. Scale bar: 6 μm. See supplementary material Movie 10.

Note that expression of the otolith protein genes *starmaker* and *otomp* was normal in MZ*ovl* and *igu* ears (supplementary material Fig. S3). In addition, mineralisation of the otoliths appeared to occur normally, as assessed by their birefringence under DIC optics (Fig. 4C,G); we never observed alternative crystal polymorphs, such as those caused by reduction of *starmaker* or *otopetrin 1* activity (Söllner et al., 2003; Hughes et al., 2004). Taken together, these data suggest that the otolith defects in MZ*ovl* and *igu* are not due to defective production of otolith components, and that cilia are not required for otolith biomineralisation.

Ciliary motility is not absolutely required for otolith formation

To test whether ciliary motility is required for otolith formation, we examined otoliths in the *lrrc50* (*dnaaf1* – Zebrafish Information Network) mutant. *lrrc50* codes for a conserved ciliary protein expressed in the ear, kidney and other ciliated tissues. In the *lrrc50* mutant, cilia have dynein arm abnormalities and are immotile; kinocilia length and number are reduced in lateral line organs (Sullivan-Brown et al., 2008; van Rooijen et al., 2008). *lrrc50* mutants were indistinguishable from siblings in fixed material (Fig. 4J), but we confirmed that otic cilia were immotile in live mutant embryos (supplementary material Movie 11; data not shown). Tether cells were present, but kinocilia were shorter than normal (supplementary material Fig. S2). As in MZ*ovl* and *igu* mutants, otoliths still formed in *lrrc50* mutants (Fig. 4K) and appeared normal in 50% (80/160) ears at 28 hpf. The remaining 50% had variable otolith defects (Fig. 4L), but some of these resolved at later stages (data not shown). These data indicate that ciliary motility is not absolutely required for otolith formation.

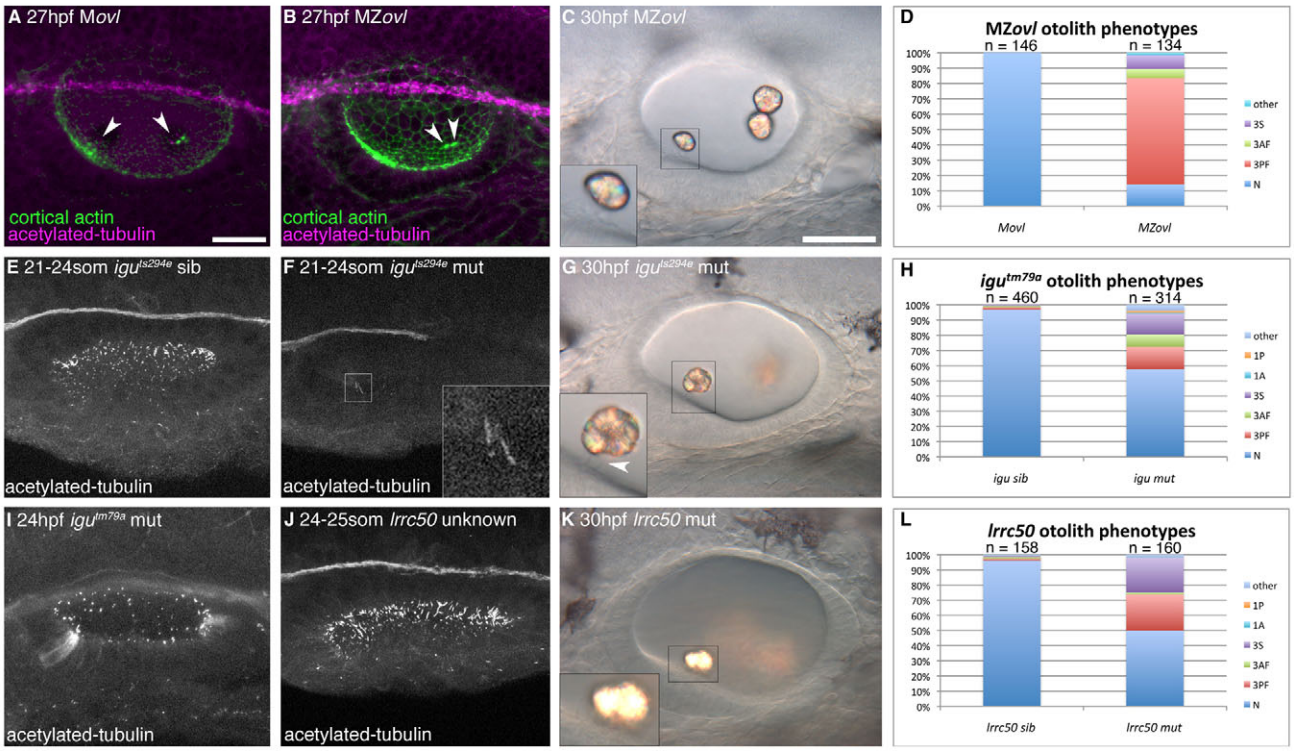

Fig. 4. Formation of otoliths in the absence of cilia. (**A**) Anti-acetylated tubulin and FITC-phalloidin stain showing tether cilia in an M*ovl* embryo (arrowheads; magenta). (**B**) MZ*ovl* mutant ears lack all cilia, but stereociliary bundles are still present (arrowheads; green). (**C**) Imperfect otoliths form in the correct position in MZ*ovl*. Inset: otolith resting directly on a stereociliary bundle. (**D**) Graph of otolith defects in MZ*ovl* embryos. (**E**) Confocal stack showing cilia in a phenotypically wild-type *igu*^{ts294e} sibling embryo. (**F**) Anterior kinocilia present in an *igu*^{ts294e} mutant (inset). (**G**) The *igu*^{ts294e} mutant lacks most cilia but still has some tether cilia (inset, arrowhead). (**H**) Graph of otolith defects in *igu*^{tm79a}. (**I**) The *igu*^{tm79a} mutant allele has more otic cilia than the *igu*^{ts294e} allele, but fewer than in wild-type embryos. (**J**) Representative confocal stack of an ear from an *lrrc50* cross. It was not possible to distinguish *lrrc50* mutant from sibling embryos at <24 hpf (*n*=15 ears). (**K**) DIC image of the ear of an *lrrc50* mutant. (**L**) Graph of *lrrc50* mutant otolith phenotypes. N, normal (two otoliths, in correct positions); 1A, one anterior otolith; 1P, one posterior otolith; 3S, three separate otoliths; 3AF, three otoliths, with two anterior otoliths fused; 3PF, three otoliths, with two posterior otoliths fused; other, other otolith defects. Scale bars: 25 μm in A, for A,B,E,F,I,J; 30 μm in C, for C,G,K.

Supernumerary kinocilia are all able to tether otolithic material

To test whether the presence of additional hair cells influences otolith nucleation, we examined otolith formation in the *mindbomb* (*mib*) mutant. *mib* codes for an E3 ubiquitin ligase required for Notch signalling (Itoh et al., 2003); in the *mib* mutant, Notch-mediated lateral inhibition fails and supernumerary hair cells form in the OV (Haddon et al., 1998). We found that all the hair cell kinocilia in *mib* were capable of binding otolith precursor particles (Fig. 5A,D; supplementary material Movie 12). The otoliths in *mib* mutants were granular in appearance, rather than a compact mass, and biomineralisation appeared to be delayed (Fig. 5B). Motile cilia were present at the poles, and in other regions of the *mib* ear, the distribution of motile and non-motile cilia appeared normal (Fig. 5D; supplementary material Movie 12).

Loss of tether cells severely disrupts otolith formation

Although otolith formation can occur in the absence of cilia, tether cells are still present in MZ*ovl* and *igu* mutants. Moreover, we observed otoliths close to the epithelium in these mutants, suggesting that they might be binding directly to the tether cell apical surface. To test whether otoliths can form in the absence of tether cells, we used a morpholino to knock down *atoh1b*, a gene required for tether cell development (Millimaki et al., 2007) (Fig. 5E-I). We confirmed the absence of tether cells and tether cilia in the ears of morphants, both in live samples (Fig. 5H; supplementary material Movie 13) and in fixed embryos (with an anti-acetylated tubulin antibody) (Fig. 5G). Unlike the loss of cilia alone, the loss of tether cells resulted in a profound disruption of otolith formation: untethered precursor particles were found throughout the OV lumen at 22S, and otolith nucleation was delayed relative to wild type (Fig. 5H; cf. Fig. 2C). At 26S, a single, untethered otolith formed (Fig. 5E). Later hair cell addition is dependent on Atoh1a (Millimaki et al., 2007) and was not affected by *atoh1b* morpholino injection. Once later hair cells had appeared, the single otolith usually became attached to hair cell kinocilia at one of the two OV poles (Fig. 5F,I) (Millimaki et al., 2007).

Extra tether cells act as otolith nucleation sites, even in the absence of cilia

The data described above suggested that the presence of tether cells, rather than the presence or motility of cilia per se, is important for otolith nucleation. We reasoned that in a mutant with extra hair cells, but lacking cilia, otolith precursor tethering to the hair cell apical surface should be even more obvious than in the MZ*ovl* mutant alone. To test this idea, we disrupted Notch

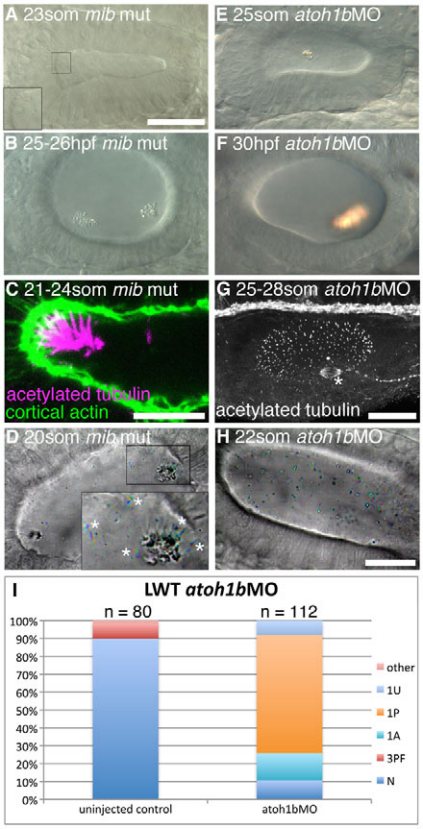

Fig. 5. Hair cells are essential for normal otolith formation. (**A**) Live image of a *mib* mutant ear at 23S. Inset: ectopic tether cilia. (**B**) Live image of a 25-26 hpf *mib* mutant ear. Otoliths do not form correctly. (**C**) Confocal image showing ectopic tether cilia in a *mib* mutant ear at 21-24S. (**D**) Time-to-colour merge of six frames from a high-speed movie of a *mib* mutant ear. Initially, all ectopic tether cilia nucleate the otolith; motile cilia are present (white asterisks). See supplementary material Movie 12. (**E**) Live image of *atoh1b*MO-injected embryo at 25S. Hair cells are absent; an untethered otolith has formed in the middle of the ear. (**F**) Live image of *atoh1b*MO-injected embryo at 30 hpf. The single otolith has become tethered to hair cell kinocilia that developed after initial otolith formation. (**G**) Confocal stack (anti-acetylated tubulin stain) showing presence of non-tether cilia in the ear of an *atoh1b* MO-injected embryo. The spindle of a dividing cell is visible (asterisk). (**H**) Time-to-colour merge of six frames of a high-speed movie of an ear from an *atoh1b* morphant embryo, showing a greater number of untethered otolith precursor particles, and absence of tether cilia and otoliths. Motile cilia are still present (*n*=3 ears; cf. Fig. 2C). See supplementary material Movie 13. (**I**) Otolith defects in the ears of *atoh1b* morphant embryos. N, normal (two otoliths, in correct positions); 1A, one anterior otolith; 1P, one posterior otolith; 1U, one untethered otolith; 3PF, three otoliths, with two posterior otoliths fused; other, other otolith defects. Scale bar: 40 μm in A, for A,B,E,F; 10 μm in C; 25 μm in G; 20 μm; in H, for D,H.

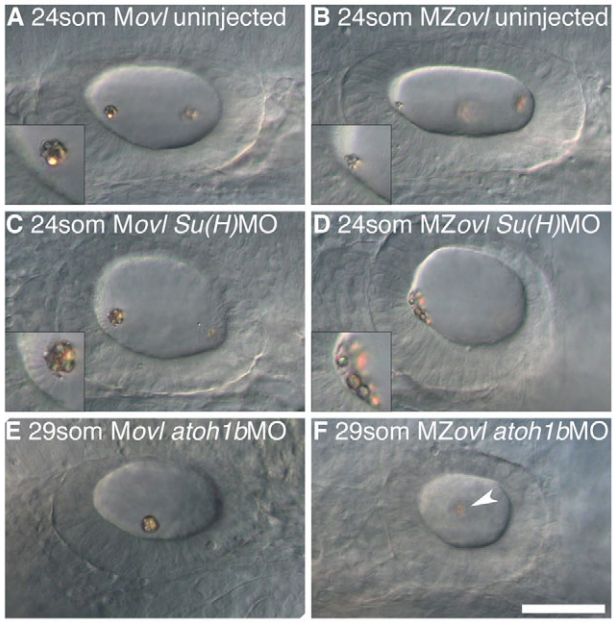

Fig. 6. The effect of ectopic hair cells and loss of hair cells on otolith formation in the absence of cilia. All panels show left ear with anterior to the left. (**A**) 24S uninjected M*ovl* control embryo; inset shows anterior otolith on tether cilia. (**B**) 24S uninjected MZ*ovl* mutant embryo; inset shows small anterior otolith tethered to the hair cells' apical surface at the anterior OV pole. (**C**) 24S M*ovl* control embryo injected with *Su(H)1+2*MO; inset shows otolith bound to several ectopic tether cilia. (**D**) 24S MZ*ovl* mutant embryo injected with *Su(H)1+2*MO; inset shows otolith precursor particles tethered to the apical surface of the ectopic hair cells. (**E**) 29S M*ovl* control embryo injected with *atoh1b*MO; one untethered otolith is present in the ear. (**F**) 29S MZ*ovl* mutant embryo injected with *atoh1b*MO; one untethered otolith (slightly out of focal plane) is present in the ear (arrowhead). The *ovl* genotype was confirmed for all samples by genotyping (data not shown). Scale bar: 40 μm for A-F.

signalling in an MZ*ovl* mutant by morpholino knockdown of both *Su(H)1* (*rbpja* – Zebrafish Information Network) and *Su(H)2* (*rbpjb* – Zebrafish Information Network) (Sieger et al., 2003; Echeverri and Oates, 2007) (Fig. 6). In a control M*ovl* embryo, the *Su(H)1+2* morpholino phenocopied the *mib* mutant ear phenotype very effectively, generating supernumerary hair cells in the ear, identified by their granular appearance and extra kinocilia (Fig. 6C). In an MZ*ovl* mutant injected with the *Su(H)1+2* morpholino, supernumerary hair cells were present, but lacked cilia. The otolith phenotype was variable, but in all cases, otolith precursor particles adhered directly to the apical surface of the epithelium in the area containing the extra hair cells (Fig. 6D; *n*=6/6). This confirmed that the hair cell apical surface can act as an otolith tethering site in the absence of cilia.

To test whether ciliary flow contributes to otolith formation in the absence of hair cells, we injected the *atoh1b* MO into MZ*ovl* mutant fish, generating an ear lacking both tether cells and cilia. In the absence of tethering sites, there was an initial disruption and delay in otolith formation, followed by the formation of a single untethered otolith in the centre of the ear (Fig. 6E,F; *n*=5/5; cf. Fig. 5E). This phenotype was indistinguishable from that of the *atoh1b* morphant alone, suggesting that in the absence of tethering sites, ciliary flow does not have a significant effect on otolith formation.

Embryo movement contributes to correct otolith nucleation

The onset of otolith formation in the ear is concomitant with the onset of muscular activity in the embryo at 18-20S. By 24 hpf, the embryo makes active turning movements within the chorion, regularly changing the position of the head with respect to gravity. Mutations affecting ciliogenesis, including *igu* and *lrrc50*, often result in a curved body axis (Brand et al., 1996; van Rooijen et al.,

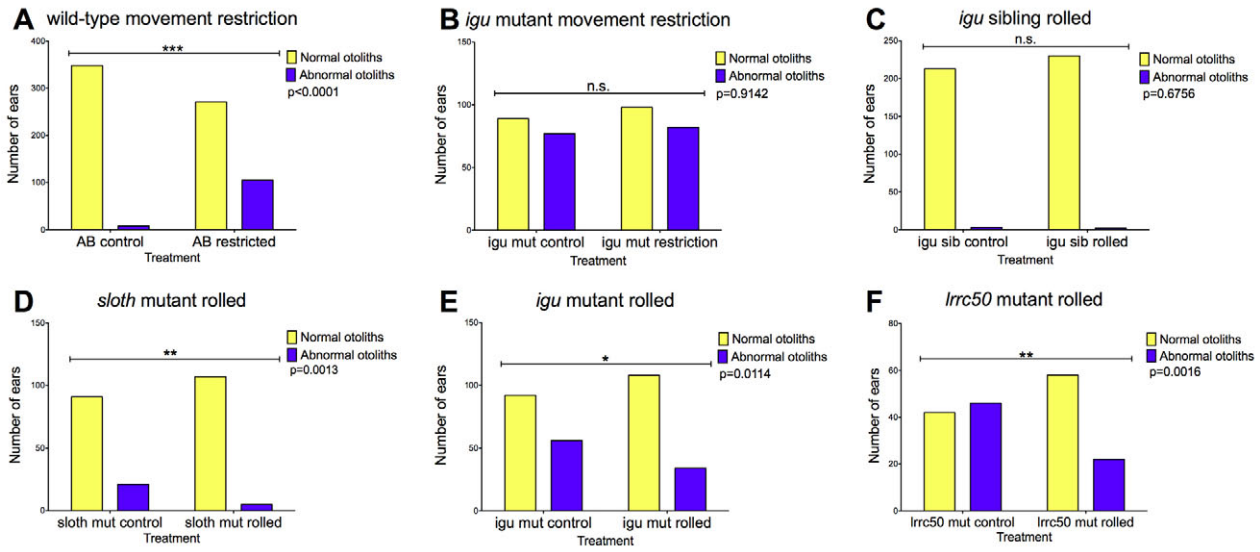

Fig. 7. Embryonic movement contributes to correct otolith formation. (**A**) Effect of restricting movement of wild-type embryos from 15-18S (before the onset of embryonic movement) for 24 hours on otolith formation. (**B**) Restricting movement of *igu*^{tm79a} mutants has no significant effect on otolith formation. (**C**) Forced motion (rolling) of phenotypically wild-type *igu* sibling embryos has no significant effect on otolith formation. (**D-F**) Rolling *sloth*, *igu*^{tm79a} and *lrrc50* mutant embryos partially rescues their otolith defects. *P* values, Fisher's exact test; n.s., not significant.

2008), which can affect embryo motility. This raised the possibility that reduced embryo movements, in addition to the ciliary defects, contribute to the otolith defects in these mutants.

To test this, we dechorionated wild-type embryos at 15-18S and raised them in methylcellulose to restrict embryonic movement. We examined otolith formation 28-30 hours later (~45 hpf). In control wild-type (AB) embryos raised in E3 alone, otolith formation is robust and reproducible; only 2.2% (8/356) of ears developed with otolith abnormalities (Fig. 7A). In embryos raised in methylcellulose, we saw an increased proportion (28%; 105/376) of ears developing with otolith defects, including those with supernumerary and fused otoliths (Fig. 7A). Development of the ear otherwise occurred normally (data not shown). We also examined otolith formation in the *sloth* (*slo*; *hsp90a*) mutant, in which embryo motility is severely impaired (Hawkins et al., 2008). About 19% (21/112) of *sloth* mutants had otolith defects (Fig. 7D). Cilia were normal, as assessed by anti-acetylated tubulin staining and high-speed video microscopy (data not shown).

To test whether enforced embryo movement can rescue otolith defects in mutants with reduced motility, we grew *igu*, *slo* and *lrrc50* mutant embryos in E3 medium that was constantly agitated on a roller from 2-3 hpf until scoring of otolith phenotypes at 30 hpf. This treatment led to a partial rescue of the otolith defects in all three mutant genotypes, whereas rolling phenotypically wild-type sibling embryos from an *igu* batch did not cause any otolith defects (Fig. 7C-F). Taken together, our data suggest that normal movements of the embryo within the chorion make a minor contribution to the process of otolith formation in the zebrafish ear.

DISCUSSION

There are at least three distinct classes of cilia in the early zebrafish otic vesicle

Previous studies have indicated that there are two classes of cilia in the early zebrafish otic vesicle (OV): short motile cilia and longer immotile tether cilia (kinocilia) (Riley et al., 1997; Yu et al., 2011). Our observations indicate that at least three forms can be distinguished (Fig. 8A). Tether cilia are present on tether cells, and readily bind otolith precursor particles (Riley et al., 1997; Tanimoto et al., 2011) (Fig. 8B,C). Tether cilia were immotile (apart from small passive displacements), as originally observed (Riley et al., 1997). Otolith binding did not trigger their immotility; tether cilia remained immotile in the *kei* mutant (this work), the *monolith* mutant (Riley et al., 1997) and the *otopetrin 1* morphant (Yu et al., 2011), all of which lack otoliths or have delayed otolith formation. However, as cilia are difficult to image at the earliest stages of OV lumen formation (18-19S), we cannot rule out the possibility that tether cilia have a transient motile stage (Fig. 8B). There have been reports of motility in kinocilia from fish ampullae under certain conditions (Bowen, 1935; Rüsch and Thurm, 1990), but this is clearly not a general phenomenon.

The tether cells at each pole were surrounded by groups of motile cilia at 21S, as has been observed previously (Wu et al., 2011; Yu et al., 2011). In general, these polar motile cilia did not bind otolithic material. Riley and colleagues were the first to observe that otolith precursor particle movement is most evident at the OV poles, in close proximity to the tether cilia (Riley et al., 1997). Polar motile cilia became shorter than the tether cilia, but persisted, beating underneath the otolith, at 24 hpf (Fig. 8D). It has been suggested that this movement contributes to the asymmetric shape of the otoliths (Wu et al., 2011).

The rest of the OV lumen was also populated by cilia, most of which were immotile. Only a few cilia (2-8% of the total, including the polar cilia) were motile, and the non-polar motile cilia were restricted to the medial wall of the OV. As we were unable to track individual cilia for more than a few seconds, we do not know whether all non-polar cilia are capable of motility, or whether there are two distinct classes (motile and non-motile) of these cilia (Fig. 8A). We did observe intermittent beating of motile cilia, which has also been reported previously (Riley et al., 1997). However, it is likely that otic cilia include non-motile primary cilia, as these are widespread throughout the embryo (Borovina et al., 2010).

It is interesting to note that motile cilia were not depleted in the *mib* mutant, even though supporting cells are absent within the sensory patches, and the extra hair cells are thought to form

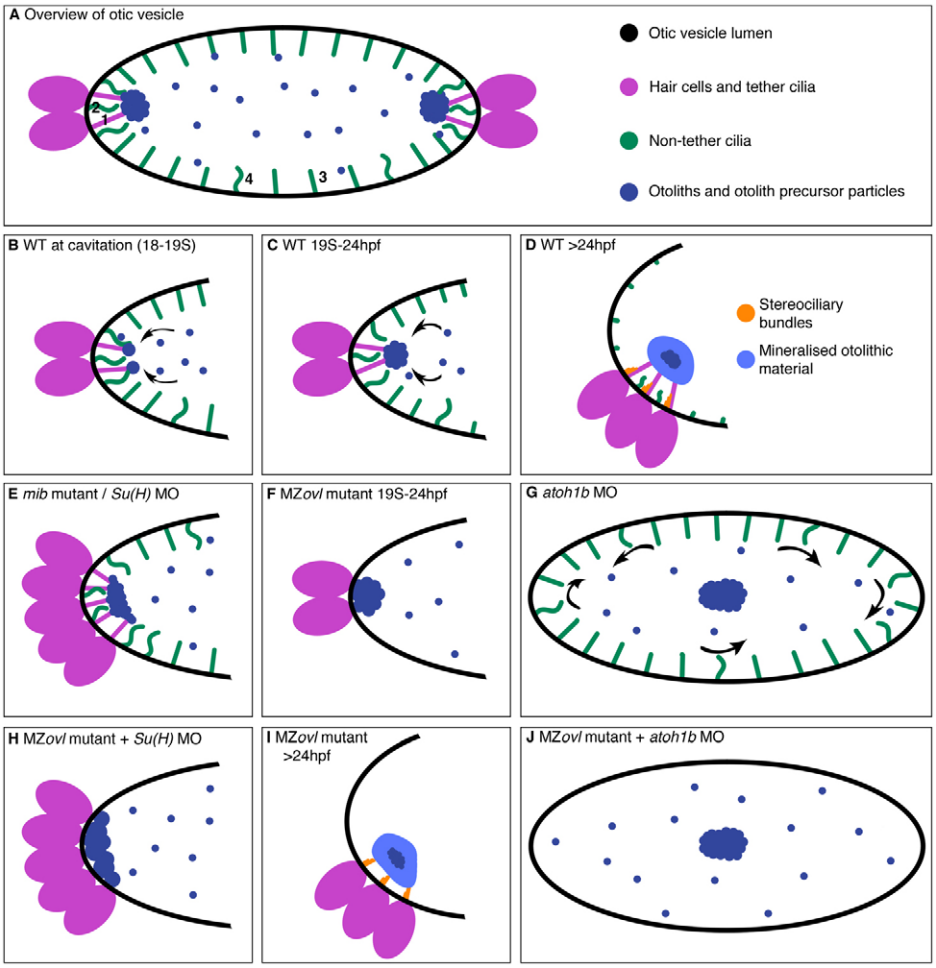

Fig. 8. Model for otolith nucleation and tethering in the zebrafish ear. (**A**) Cartoon overview of the OV between 19 and 24 hpf. Four ciliary classes are labelled: immotile tether cilia (1), polar motile cilia (2), immotile non-polar cilia lining the OV lumen (3), and occasional motile cilia on the medial wall (4). (**B-D**) Stage series showing proposed mechanism of otolith nucleation in wild-type embryos. (**E**) In *mib* mutants, ectopic hair cell tether cilia initially nucleate a flatter otolith. (**F**) In MZ*ovl* mutants, which lack all cilia, otolith precursor particles attach directly to the hair cell apical surface. (**G**) In the absence of hair cells (*atoh1b*MO), otolith precursor particles form a single untethered otolith. (**H**) In an ear with supernumerary hair cells but lacking cilia [MZ*ovl* + *Su(H)1+2*MO], otolith precursor particles bind over a wide area at the OV poles. (**I**) At 24 hpf, the otolith binds directly to hair cell stereocilia in an MZ*ovl* mutant. (**J**) In an ear lacking both hair cells and cilia (MZ*ovl* + *atoh1b*MO), an untethered otolith forms, as for *atoh1b*MO alone (G). See also supplementary material Table S1.

at the expense of supporting cells (Haddon et al., 1998; Haddon et al., 1999). If supporting cells bear motile cilia, our data suggest that some supporting cells remain at the periphery of the sensory patches in *mib* mutants. Alternatively, the cells with motile cilia might represent a third cell type in the sensory patch, in addition to hair cells and supporting cells. At later stages, otolith growth is slow in *mib* mutants, probably owing to the paucity of supporting cells, which are thought to provide components for otolith growth and biomineralisation (Haddon et al., 1999).

Otoliths can form in the absence of cilia or ciliary motility

The correlation between otolith defects and ciliary dysfunction in the zebrafish is well documented (Panizzi et al., 2007; Colantonio et al., 2009; Neugebauer et al., 2009; Serluca et al., 2009; Wilkinson et al., 2009; Gao et al., 2010; Yu et al., 2011). Nevertheless, the complete loss of cilia causes surprisingly mild otolith defects. Otoliths were still present in mutants lacking or with reduced numbers of cilia, and in about 14% of MZ*ovl* and 56% of *igu* mutants, otoliths appeared to develop normally. In wild-type embryos, otolith precursor particles clearly nucleate at the tips of the tether cilia (Haddon and Lewis, 1996), and indeed are so strongly bound to them that they cannot be dislodged with laser tweezers (Riley et al., 1997). These observations indicate that any otolith precursor-binding factor must normally be localised to the tips of the kinocilia. However, the presence and tethering of otoliths in mutants lacking cilia (*MZovl*) or with fewer tether cilia (*igu*) indicates that cilia are not absolutely necessary for otolith formation and tethering at the poles of the ear.

Likewise, disruption of ciliary motility results in only mild otolith defects; ~50% of *lrrc50* mutant ears developed with normal otoliths, and otolith development was perturbed, but not absent, in morphants for the ciliary motility genes *gas8* (Colantonio et al., 2009) and *foxj1b* (Yu et al., 2011). Taken together, these data suggest that even when movement of otolith precursor particles is diffusion-limited, otolith tethering at the OV poles can still occur. Precursor particles readily adhere to one another when brought into contact artificially, and it has been suggested that ciliary movement ensures the even distribution of precursor particles and prevents their premature aggregation (Riley et al., 1997). However, we have not found evidence for premature aggregation of otolith precursor particles in the absence of ciliary movement, either in the presence or absence of hair cells. Normal ciliary movement was not sufficient to prevent the late ectopic otolith aggregation in the centre of the OV in the absence of hair cells (*atoh1b* morphant), which occurs whether or not cilia are present. Nevertheless, the presence of ectopic motile cilia, caused by over-expression of *foxj1b*, can disrupt otolith formation (Yu et al., 2011). We conclude that, although tether cilia clearly provide the normal site for otolith nucleation, and ciliary motility ensures the accuracy and robustness of this process, the presence and motility of cilia is not as crucial for otolith formation as is the presence of tether cells.

Embryonic movements make a minor contribution to correct otolith formation

When embryonic movement was restricted (either genetically or physically), embryos developed with minor otolith defects. Impaired embryo movement might, therefore, contribute to the otolith defects in embryos with defective cilia, as these mutants invariably have a curved body axis and reduced movement (Brand et al., 1996; Tsujikawa and Malicki, 2004; Kramer-Zucker et al., 2005; van Rooijen et al., 2008; Wilkinson et al., 2009; Clément et al., 2011). Moreover, otolith defects were partially rescued when ciliary mutants were raised under constant agitation. However, the proportion of otolith defects in ciliary mutants was greater than that in wild-type embryos grown in methylcellulose, and restricting movement of *igu* mutants did not strengthen their otolith phenotype. These results suggest that embryonic movement plays only a minor role in normal otolith formation. A previous study reported that immobilising wild-type embryos with the embryo oriented vertically does not affect otolith development (Riley et al., 1997). Variations in staging, timing or orientation might account for the differences between this and our observations. Embryonic movement did not appear to be affected in our *atoh1b* morphants, and so is not sufficient to rescue otolith formation in the absence of tether cells.

An otolith precursor-binding factor?

Unlike cilia, tether cells are essential for correct otolith nucleation, as shown by the severe disruption to otolith formation in the *atoh1b* morphant. Otolith precursor particles were present, indicating that tether cells are not the sole source of precursor particle material, but the process of nucleation was severely delayed. This result supports the existence of an otolith precursor-binding factor [originally proposed by Riley et al. (Riley et al., 1997)] that is synthesised by tether cells and normally localised to the tips of their kinocilia. If ectopic hair cells are present [*mib* mutant or *Su(H)1+2* morphant], all produce the binding factor, and precursor particles adhere to the tips of all the kinocilia. In the absence of tether cilia (MZ*ovl*), we hypothesise that the factor is still made, enabling precursor particles to nucleate directly to the tether cell apical surface. This was demonstrated most dramatically in the MZ*ovl* mutant injected with the *Su(H)1+2* morpholino; otolith precursor particles bound over a wider area to the apical surfaces of the supernumerary hair cells. It is likely that the factor also localises to stereocilia, at least in the absence of cilia, as the otoliths in *MZovl* mutants sit directly on the stereocilia at 24 hpf (Fig. 4C; Fig. 8I). Direct tethering to the hair cell surface also occurs in *igu* mutant ears (this work) (Yu et al., 2011) when tether cilia are missing. In the absence of tether cells (*atoh1b* morphant), we hypothesise that the factor is no longer expressed in the early OV, resulting in a delay in otolith nucleation and loss of tethering (Fig. 8E-G).

The identity of the otolith precursor-binding factor is not yet known, but as otolith precursor particles are thought to contain glycogen (Pisam et al., 2002), proteins containing glycogen-binding domains (Machovič and Janeček, 2006) provide good candidates. Another proposed candidate is an integrin-like protein, for interaction with the RGD peptide in osteopontin, a known component of mammalian otoconia (Riley et al., 1997; Sumanas et al., 2003). A molecule that might be involved in production or assembly of the otolith precursor-binding factor is the chaperone protein Hsp90β1. Morpholinos to *hsp90b1* phenocopy the otolith defects seen in *atoh1b* morphants, with a delay in otolith nucleation and the presence of precursor particles throughout the OV at 21 hpf (Sumanas et al., 2003). Importantly, however, tether cells and cilia are still present in *hsp90b1* morphants, and ciliary movement is thought to be normal. As in *atoh1b* morphants, precursor particles eventually coalesce into a single otolith, which becomes tethered to hair cell kinocilia at one of the two poles (Sumanas et al., 2003). Hsp90β1 is unlikely to be the otolith-binding factor itself, as it is localised to the endoplasmic reticulum.

Although the otolith precursor-binding factor is required during the initial stages of otolith formation, it is likely that the mechanisms of otolith tethering change as development proceeds. The otolith becomes biomineralised and must also become embedded in the otolithic membrane, a gelatinous matrix that mechanically couples the otolith to the sensory epithelium beneath (reviewed by Gauldie and Nelson, 1990; Hughes et al., 2006). Little is known about the otolithic membrane in zebrafish; it is not present prior to 27 hpf (Tanimoto et al., 2011), but has been visualised as a fibrous network by scanning electron microscopy at 4 days post fertilisation (Hughes et al., 2004). It is likely to contain the collagen-like protein Otolin 1 (Murayama et al., 2005), a known component of the otolithic membrane in fish, and the otoconial membrane in mammals (Deans et al., 2010). Identification of the otolith precursor-binding factor, together with further characterisation of the otolithic membrane, will be important for a full understanding of the tethering, growth and function of the otoliths in the zebrafish ear.

Acknowledgements

We thank Soheil Aghamohammadzadeh for help with confocal microscopy; Sara Solaymani-Kohal and Tim Chico for help with high-speed video microscopy; and Andrew Furley and Bruce Riley for helpful discussion. We are grateful to Freek van Eeden, Brian Ciruna, Carole Wilson and Steve Wilson for providing mutant and transgenic lines; Freek van Eeden and Robert Wilkinson for the *Su(H)1+2* morpholino; other members of the zebrafish community for providing probes; and the aquarium staff for expert care of the zebrafish.

Funding

This work was supported by grants from the Biotechnology and Biological Sciences Research Council (BBSRC) [BB/F017588/1, BB/E015875/1 to T.T.W.] and from the Muscular Dystrophy Association [to P.H. and A.F.S.]. The Medical Research Council (MRC) Centre for Developmental and Biomedical Genetics (CDBG) zebrafish aquaria and imaging facilities were supported by the MRC [G0700091] and Wellcome Trust [GR077544AIA]. Deposited in PMC for release after 6 months.

Competing interests statement

The authors declare no competing financial interests.

Supplementary material

Supplementary material available online at
http://dev.biologists.org/lookup/suppl/doi:10.1242/dev.079947/-/DC1

References

Abbas, L. and Whitfield, T. T. (2010). The zebrafish inner ear. In *Zebrafish*, Vol. 29 (ed. S. F. Perry, M. Ekker, A. P. Farrell and C. J. Brauner). London, UK: Academic Press.

Becker-Heck, A., Zohn, I. E., Okabe, N., Pollock, A., Lenhart, K. B., Sullivan-Brown, J., McSheene, J., Loges, N. T., Olbrich, H., Haeffner, K. et al. (2011). The coiled-coil domain containing protein CCDC40 is essential for motile cilia function and left-right axis formation. *Nat. Genet.* **43**, 79-84.

Bisgrove, B. W. and Yost, H. J. (2006). The roles of cilia in developmental disorders and disease. *Development* **133**, 4131-4143.

Bisgrove, B. W., Snarr, B. S., Emrazian, A. and Yost, H. J. (2005). Polaris and Polycystin-2 in dorsal forerunner cells and Kupffer's vesicle are required for specification of the zebrafish left-right axis. *Dev. Biol.* **287**, 274-288.

Borovina, A., Superina, S., Voskas, D. and Ciruna, B. (2010). Vangl2 directs the posterior tilting and asymmetric localization of motile primary cilia. *Nat. Cell Biol.* **12**, 407-412.

Bowen, R. E. (1935). Movement of sensory hairs in the ear. *Proc. Natl. Acad. Sci. USA* **21**, 233-234.
Brand, M., Heisenberg, C.-P., Warga, R. M., Pelegri, F., Karlstrom, R. O., Beuchle, D., Picker, A., Jiang, Y.-J., Furutani-Seiki, M., van Eeden, F. J. M. et al. (1996). Mutations affecting development of the midline and general body shape during zebrafish embryogenesis. *Development* **123**, 129-142.
Clément, A., Solnica-Krezel, L. and Gould, K. L. (2011). The Cdc14B phosphatase contributes to ciliogenesis in zebrafish. *Development* **138**, 291-302.
Colantonio, J. R., Vermot, J., Wu, D., Langenbacher, A. D., Fraser, S., Chen, J. N. and Hill, K. L. (2009). The dynein regulatory complex is required for ciliary motility and otolith biogenesis in the inner ear. *Nature* **457**, 205-209.
Deans, M. R., Peterson, J. M. and Wong, G. W. (2010). Mammalian Otolin: a multimeric glycoprotein specific to the inner ear that interacts with otoconial matrix protein Otoconin-90 and Cerebellin-1. *PLoS ONE* **5**, e12765.
Echeverri, K. and Oates, A. C. (2007). Coordination of symmetric cyclic gene expression during somitogenesis by Suppressor of Hairless involves regulation of retinoic acid catabolism. *Dev. Biol.* **301**, 388-403.
Gao, C., Wang, G., Amack, J. D. and Mitchell, D. R. (2010). Oda16/Wdr69 is essential for axonemal dynein assembly and ciliary motility during zebrafish embryogenesis. *Dev. Dyn.* **239**, 2190-2197.
Gauldie, R. W. and Nelson, D. G. A. (1990). Otolith growth in fishes. *Comp. Biochem. Physiol.* **97A**, 119-135.
Glazer, A. M., Wilkinson, A. W., Backer, C. B., Lapan, S. W., Gutzman, J. H., Cheeseman, I. M. and Reddien, P. W. (2010). The Zn finger protein Iguana impacts Hedgehog signaling by promoting ciliogenesis. *Dev. Biol.* **337**, 148-156.
Granato, M., van Eeden, F. J. M., Schach, U., Trowe, T., Brand, M., Furutani-Seiki, M., Haffter, P., Hammerschmidt, M., Heisenberg, C.-P., Jiang, Y.-J. et al. (1996). Genes controlling and mediating locomotion behavior of the zebrafish embryo and larva. *Development* **123**, 399-413.
Haddon, C. and Lewis, J. (1996). Early ear development in the embryo of the zebrafish, *Danio rerio*. *J. Comp. Neurol.* **365**, 113-123.
Haddon, C., Jiang, Y.-J., Smithers, L. and Lewis, J. (1998). Delta-Notch signalling and the patterning of sensory cell differentiation in the zebrafish ear: evidence from the *mind bomb* mutant. *Development* **125**, 4637-4644.
Haddon, C., Mowbray, C., Whitfield, T., Jones, D., Gschmeissner, S. and Lewis, J. (1999). Hair cells without supporting cells: further studies in the ear of the zebrafish *mind bomb* mutant. *J. Neurocytol.* **28**, 837-850.
Hammond, K. L., Loynes, H. E., Folarin, A. A., Smith, J. and Whitfield, T. T. (2003). Hedgehog signalling is required for correct anteroposterior patterning of the zebrafish otic vesicle. *Development* **130**, 1403-1417.
Hawkins, T. A., Haramis, A. P., Etard, C., Prodromou, C., Vaughan, C. K., Ashworth, R., Ray, S., Behra, M., Holder, N., Talbot, W. S. et al. (2008). The ATPase-dependent chaperoning activity of Hsp90a regulates thick filament formation and integration during skeletal muscle myofibrillogenesis. *Development* **135**, 1147-1156.
Huang, P. and Schier, A. F. (2009). Dampened Hedgehog signaling but normal Wnt signaling in zebrafish without cilia. *Development* **136**, 3089-3098.
Hughes, I., Blasiole, B., Huss, D., Warchol, M. E., Rath, N. P., Hurle, B., Ignatova, E., Dickman, J. D., Thalmann, R., Levenson, R. et al. (2004). Otopetrin 1 is required for otolith formation in the zebrafish *Danio rerio*. *Dev. Biol.* **276**, 391-402.
Hughes, I., Thalmann, I., Thalmann, R. and Ornitz, D. M. (2006). Mixing model systems: Using zebrafish and mouse inner ear mutants and other organ systems to unravel the mystery of otoconial development. *Brain Research* **1091**, 58-74.
Ishikawa, H. and Marshall, W. F. (2011). Ciliogenesis: building the cell's antenna. *Nat. Rev. Mol. Cell Biol.* **12**, 222-234.
Itoh, M., Kim, C. H., Palardy, G., Oda, T., Jiang, Y.-J., Maust, D., Yeo, S. Y., Lorick, K., Wright, G. J., Ariza-McNaughton, L. et al. (2003). Mind bomb is a ubiquitin ligase that is essential for efficient activation of Notch signaling by Delta. *Dev. Cell* **4**, 67-82.
Jiang, Y.-J., Brand, M., Heisenberg, C.-P., Beuchle, D., Furutani-Seiki, M., Kelsh, R. N., Warga, R. M., Granato, M., Haffter, P., Hammerschmidt, M. et al. (1996). Mutations affecting neurogenesis and brain morphology in the zebrafish, *Danio rerio*. *Development* **123**, 205-216.
Kang, N., Ro, H., Park, Y., Kim, H. T., Huh, T. L. and Rhee, M. (2010). Seson, a novel zinc finger protein, controls cilia integrity for the LR patterning during zebrafish embryogenesis. *Biochem. Biophys. Res. Commun.* **401**, 169-174.
Kim, H. R., Richardson, J., van Eeden, F. and Ingham, P. W. (2010). Gli2a protein localization reveals a role for Iguana/DZIP1 in primary ciliogenesis and a dependence of Hedgehog signal transduction on primary cilia in the zebrafish. *BMC Biology* **19**, 65.
Kimmel, C. B., Ballard, W. W., Kimmel, S. R., Ullmann, B. and Schilling, T. F. (1995). Stages of embryonic development of the zebrafish. *Dev. Dyn.* **203**, 253-310.
Kramer-Zucker, A. G., Olale, F., Haycraft, C. J., Yoder, B. K., Schier, A. F. and Drummond, I. A. (2005). Cilia-driven fluid flow in the zebrafish pronephros, brain and Kupffer's vesicle is required for normal organogenesis. *Development* **132**, 1907-1921.
Machovič, M. and Janeček, S. (2006). The evolution of putative starch-binding domains. *FEBS Lett.* **580**, 6349-6356.
Malicki, J., Schier, A. F., Solnica-Krezel, L., Stemple, D. L., Neuhauss, S. C. F., Stainier, D. Y. R., Abdelilah, S., Rangini, Z., Zwartkruis, F. and Driever, W. (1996). Mutations affecting development of the zebrafish ear. *Development* **123**, 275-283.
May-Simera, H. L., Kai, M., Hernandez, V., Osborn, D. P., Tada, M. and Beales, P. L. (2010). Bbs8, together with the planar cell polarity protein Vangl2, is required to establish left-right asymmetry in zebrafish. *Dev. Biol.* **345**, 215-225.
Millimaki, B. B., Sweet, E. M., Dhason, M. S. and Riley, B. B. (2007). Zebrafish *atoh1* genes: classic proneural activity in the inner ear and regulation by Fgf and Notch. *Development* **134**, 295-305.
Murayama, E., Herbomel, P., Kawakami, A., Takeda, H. and Nagasawa, H. (2005). Otolith matrix proteins OMP-1 and Otolin-1 are necessary for normal otolith growth and their correct anchoring onto the sensory maculae. *Mech. Dev.* **122**, 791-803.
Neugebauer, J. M., Amack, J. D., Peterson, A. G., Bisgrove, B. W. and Yost, H. J. (2009). FGF signalling during embryo development regulates cilia length in diverse epithelia. *Nature* **458**, 651-654.
Omori, Y. and Malicki, J. (2006). *oko meduzy* and related *crumbs* genes are determinants of apical cell features in the vertebrate embryo. *Curr. Biol.* **16**, 945-957.
Omori, Y., Zhao, C., Saras, A., Mukhopadhyay, S., Kim, W., Furukawa, T., Sengupta, P., Veraksa, A. and Malicki, J. (2008). *elipsa* is an early determinant of ciliogenesis that links the IFT particle to membrane-associated small GTPase Rab8. *Nat. Cell Biol.* **10**, 437-444.
Panizzi, J. R., Jessen, J. R., Drummond, I. A. and Solnica-Krezel, L. (2007). New functions for a vertebrate Rho guanine nucleotide exchange factor in ciliated epithelia. *Development* **134**, 921-931.
Pathak, N., Obara, T., Mangos, S., Liu, Y. and Drummond, I. A. (2007). The zebrafish *fleer* gene encodes an essential regulator of cilia tubulin polyglutamylation. *Mol. Biol. Cell* **18**, 4353-4364.
Pathak, N., Austin, C. and Drummond, I. A. (2011). Tubulin tyrosine ligase like genes TTLL3 and TTLL6 maintain zebrafish cilia structure and motility. *J. Biol. Chem.* **286**, 11685-11695.
Pisam, M., Jammet, C. and Laurent, D. (2002). First steps of otolith formation of the zebrafish: role of glycogen? *Cell Tissue Res.* **310**, 163-168.
Popper, A. N. and Fay, R. R. (1999). The auditory periphery in fishes. In *Comparative hearing: fish and amphibians*, vol. 11 (ed. R. R. Fay and A. N. Popper). New York: Springer Verlag.
Popper, A. N. and Lu, Z. (2000). Structure-function relationships in fish otolith organs. *Fisheries Research* **46**, 15-25.
Ravanelli, A. M. and Klingensmith, J. (2011). The actin nucleator Cordon-bleu is required for development of motile cilia in zebrafish. *Dev. Biol.* **350**, 101-111.
Riley, B. B., Zhu, C., Janetopoulos, C. and Aufderheide, K. J. (1997). A critical period of ear development controlled by distinct populations of ciliated cells in the zebrafish. *Dev. Biol.* **191**, 191-201.
Rothschild, S. C., Francescatto, L., Drummond, I. A. and Tombes, R. M. (2011). CaMK-II is a PKD2 target that promotes pronephric kidney development and stabilizes cilia. *Development* **138**, 3387-3397.
Rüsch, A. and Thurm, U. (1990). Spontaneous and electrically induced movements of ampullary kinocilia and stereovilli. *Hear. Res.* **48**, 247-263.
Sekimizu, K., Nishioka, N., Sasaki, H., Takeda, H., Karlstrom, R. O. and Kawakami, A. (2004). The zebrafish *iguana* locus encodes Dzip1, a novel zinc-finger protein required for proper regulation of Hedgehog signaling. *Development* **131**, 2521-2532.
Serluca, F. C., Xu, B., Okabe, N., Baker, K., Lin, S. Y., Sullivan-Brown, J., Konieczkowski, D. J., Jaffe, K. M., Bradner, J. M., Fishman, M. C. et al. (2009). Mutations in zebrafish leucine-rich repeat-containing six-like affect cilia motility and result in pronephric cysts, but have variable effects on left-right patterning. *Development* **136**, 1621-1631.
Sieger, D., Tautz, D. and Gajewski, M. (2003). The role of *Suppressor of Hairless* in Notch mediated signalling during zebrafish somitogenesis. *Mech. Dev.* **120**, 1083-1094.
Söllner, C., Burghammer, M., Busch-Nentwich, E., Berger, J., Schwartz, H., Riekel, C. and Nicolson, T. (2003). Control of crystal size and lattice formation by Starmaker in otolith biomineralization. *Science* **302**, 282-286.
Sullivan-Brown, J., Schottenfeld, J., Okabe, N., Hostetter, C. L., Serluca, F. C., Thiberge, S. Y. and Burdine, R. D. (2008). Zebrafish mutations affecting cilia motility share similar cystic phenotypes and suggest a mechanism of cyst formation that differs from *pkd2* morphants. *Dev. Biol.* **314**, 261-275.
Sumanas, S., Larson, J. D. and Bever, M. M. (2003). Zebrafish chaperone protein GP96 is required for otolith formation during ear development. *Dev. Biol.* **261**, 443-455.
Tanimoto, M, Ota, Y., Inoue, M. and Oda, Y. (2011). Origin of inner ear hair cells: morphological and functional differentiation from ciliary cells into hair cells in zebrafish inner ear. *J. Neurosci.* **31**, 3784-3794.

Tay, S. Y., Yu, X., Wong, K. N., Panse, P., Ng, C. P. and Roy, S. (2010). The iguana/DZIP1 protein is a novel component of the ciliogenic pathway essential for axonemal biogenesis. *Dev. Dyn.* **239**, 527-534.

Tsujikawa, M. and Malicki, J. (2004). Intraflagellar transport genes are essential for differentiation and survival of vertebrate sensory neurons. *Neuron* **42**, 703-716.

van Rooijen, E., Giles, R. H., Voest, E. E., van Rooijen, C., Schulte-Merker, S. and van Eeden, F. J. (2008). LRRC50, a conserved ciliary protein implicated in polycystic kidney disease. *J. Am. Soc. Nephrol.* **19**, 1128-1138.

Westerfield, M. (2000). *The Zebrafish Book. A Guide for the Laboratory Use of Zebrafish (Danio rerio)*. Eugene: University of Oregon Press.

Whitfield, T. T., Granato, M., van Eeden, F. J. M., Schach, U., Brand, M., Furutani-Seiki, M., Haffter, P., Hammerschmidt, M., Heisenberg, C.-P., Jiang, Y.-J. et al. (1996). Mutations affecting development of the zebrafish inner ear and lateral line. *Development* **123**, 241-254.

Wilkinson, C. J., Carl, M. and Harris, W. A. (2009). Cep70 and Cep131 contribute to ciliogenesis in zebrafish embryos. *BMC Cell Biol.* **10**, 17.

Wolff, C., Roy, S., Lewis, K. E., Schauerte, H., Joerg-Rauch, G., Kirn, A., Weiler, C., Geisler, R., Haffter, P. and Ingham, P. W. (2004). *iguana* encodes a novel zinc-finger protein with coiled-coil domains essential for Hedgehog signal transduction in the zebrafish embryo. *Genes Dev.* **18**, 1565-1576.

Wu, D., Freund, J. B., Fraser, S. E. and Vermot, J. (2011). Mechanistic basis of otolith formation during teleost inner ear development. *Dev. Cell* **20**, 271-278.

Xiao, T., Roeser, T., Staub, W. and Baier, H. (2005). A GFP-based genetic screen reveals mutations that disrupt the architecture of the zebrafish retinotectal projection. *Development* **132**, 2955-2967.

Yu, X., Ng, C. P., Habacher, H. and Roy, S. (2008). Foxj1 transcription factors are master regulators of the motile ciliogenic program. *Nat. Genet.* **40**, 1445-1453.

Yu, X., Lau, D., Ng, C. P. and Roy, S. (2011). Cilia-driven fluid flow as an epigenetic cue for otolith biomineralization on sensory hair cells of the inner ear. *Development* **138**, 487-494.